

## Direct laser writing of three-dimensional photonic structures in Nd:yttrium aluminum garnet laser ceramics

Airán Ródenas,<sup>1,a)</sup> Guangyong Zhou,<sup>2</sup> Daniel Jaque,<sup>1</sup> and Min Gu<sup>2,b)</sup>

<sup>1</sup>*GIEL, Departamento de Física de Materiales C-IV, Facultad de Ciencias, Universidad Autónoma de Madrid, 28049 Madrid, Spain*

<sup>2</sup>*Centre for Micro-Photonics and Centre for Ultrahigh-bandwidth Devices for Optical Systems, Faculty of Engineering and Industrial Sciences, Swinburne University of Technology, P. O. Box 218, Hawthorn, Victoria 3122, Australia*

(Received 9 May 2008; accepted 16 September 2008; published online 14 October 2008)

We report on the direct laser writing of a three-dimensional photonic structure in a neodymium doped yttrium aluminum garnet laser ceramic. The fabricated structure consists of a voxel-based face centered cubic lattice showing a stop band centered at 2.4  $\mu\text{m}$ . Confocal luminescence imaging was used to study the submicron low refractive-index voxels constituting the photonic structure, as well as to elucidate how the luminescence properties of the neodymium laser ions are modified by the writing process. © 2008 American Institute of Physics. [DOI: 10.1063/1.2998258]

A great scientific effort has been done since, more than 2 decades ago, a pioneering work of Purcell<sup>1</sup> started to attract the attention of researchers.<sup>2,3</sup> The race for the achievement of a real control over the light flow rapidly encountered serious technological challenges, which delayed for almost one decade the demonstration of two- and three-dimensional (2D and 3D) photonic crystals (PhCs).<sup>4,5</sup> Since then, the 3D periodic structuring has continued to be a challenging and elusive goal. Although the feasibility of 3D PhC structures in the optical range has been demonstrated by combining different approaches<sup>4,6,7</sup> the direct laser writing (DLW) technique is emerging as one of the most promising ones since it is a direct, fast and cost-effective fabrication method.<sup>8-10</sup>

In order to build-up a PhC it is necessary to tailor both the geometry of the structure and the refractive-index change modulation. When applied to dielectric materials, the DLW technique consists the creation of localized laser-induced submicron explosions inside bulk medium. The tightly confined dielectric breakdown develops after relaxation in a low refractive-index voxel,<sup>11,12</sup> and subsequently entails several relaxation processes which can leave a signature in the crystalline surroundings.<sup>13</sup> The voxel-based DLW technique has been previously proved to be an efficient method for fabricating 3D PhCs in several kinds of undoped glasses,<sup>10</sup> polymers,<sup>14</sup> and lithium niobate crystals.<sup>15</sup> Since research on photonic band engineering is believed to hold the key for the next generation of photonic devices,<sup>16</sup> the possibility of achieving it on crystalline laser media is of special relevance.

Rare earth ions, such as neodymium ( $\text{Nd}^{3+}$ ) ions, possess specific features which are important in the context of spontaneous emission engineering; featuring high luminescence efficiencies, narrow emission bands, as well as rigidly fixed locations in specific local sites of the matrix.<sup>17</sup> Despite its technological interest, the creation of 3D PhCs in rare earth doped dielectric media has not, up until now, been demonstrated yet.

In this letter we examine the possibility of DLW a 3D photonic structure in a  $\text{Nd}^{3+}$  doped fine-grain yttrium aluminum garnet transparent ceramic (hereafter Nd:cYAG).

Nd:cYAG is one of the most promising materials in the field of photonic laser technology since it combines the unique laser properties of Nd:YAG crystals with the large-scale, flexible, and cost-effective production processes of ceramics.<sup>18</sup> Transmission confocal laser scanning microscopy (CLSM) and time-resolved confocal luminescence mapping were also used in order to characterize the submicron voxel shapes and the luminescence properties of the  $\text{Nd}^{3+}$  ions inside the photonic structure.

The experimental setup consists of a chirped pulse amplified Ti:sapphire femtosecond laser (Spitfire, Spectra Physics) providing 60 fs, 800 nm wavelength, linearly polarized pulses at a repetition rate of 1 KHz. The laser radiation was focused by an Olympus PlanAPO  $60\times 1.4$  numerical aperture (NA) oil immersion objective. The Nd:cYAG sample [provided by Baikowski Ltd. (Japan) with a nominal  $\text{Nd}^{3+}$  concentration of 1 at. %, and index of refraction  $n=1.82$ ] was mounted on a 3D nanopositioning stage (PI, Germany). More details about the experimental setup can be found elsewhere.<sup>15</sup> 3D writing of a photonic band gap structure requires the creation of voxels at different depths inside the transparent medium with controlled shape and optical contrast. In order to reach such a control, it is necessary to previously investigate how the laser-photomodification and the high-NA optical aberration processes combine. Figure 1(a) shows some submicron and micrometer sized voxels produced when varying the depth and energy writing parameters, as measured by CLSM.

After a detailed study we were able to find, for each depth inside the sample, the laser power leading to a best compromise between voxel size and magnitude of the induced refractive-index change. Figure 1(b) shows the CLSM side views of different submicron voxels corresponding to different layers of the photonic structure. The transversal size of the written voxels can be estimated from these pictures. For a depth of 6  $\mu\text{m}$  we can obtain the shape factor of  $\sim 1.1$  with lateral and axial sizes of  $\sim 495$  and  $\sim 532$  nm, respectively. This quasispherical shape can be reasonably kept all through deeper layers inside the sample at the expense of gradually losing refractive-index contrast. Once the optimal writing conditions were determined, a 35-layer face centered cubic (fcc) structure with a lattice constant of 1  $\mu\text{m}$  was fabricated. Laser energy was varied from 40 to 80  $\mu\text{W}$  for

<sup>a)</sup>Electronic mail: airan.rodenas@uam.es.

<sup>b)</sup>Electronic mail: mgu@groupwise.swin.edu.au.

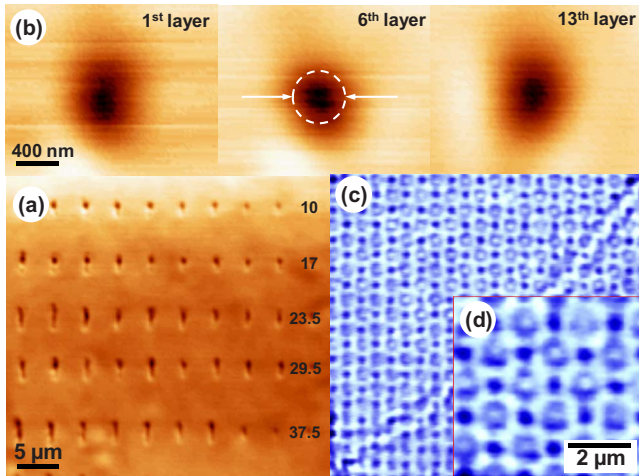


FIG. 1. (Color online) (a) Voxel shapes for different writing depths and laser energies as obtained from the [010] direction transmission CLSM images. (b) Lateral CLSM images of three voxels with the approximate same shape at 6, 11, and 18  $\mu\text{m}$  depths (1st, 6th, and 13th layers, respectively). (c) Micrograph image of the written structure and (d) detail of the fcc structure from the top view ([100] direction).

the first and last layers, respectively; the number of laser pulses per lattice point was fixed to 50. The first and last layers were located at 6 and 40  $\mu\text{m}$  from surface, respectively. Figure 1(c) shows the micrograph image of the obtained structure when focusing at the second layer from surface. An enhanced detail of the image [Fig. 1(d)] reveals the fcc structure with the first layer voxels defocused, and the second layer voxels focused.

The photonic properties of the structure were examined by accurately measuring the transmission spectra along the [100] direction. Setup details can be found elsewhere.<sup>19</sup> Figure 2 shows a measured transmission spectrum, which displays a stop band centered at 2.4  $\mu\text{m}$  with a rather weak suppression rate of  $\sim 5\%$ . This result was consistent when measured at different positions of the sample, and disappeared for higher layer-spacing structures. Simulation (not shown) with commercial RSOFT software predicted a narrow fundamental stop gap very sensitive to the measuring direction. For the experimental angular distribution of our setup ( $\sim 8^\circ$ ) simulations predict a midgap position lying between 3.57 and 2.29  $\mu\text{m}$ , thus consistent with the experimental re-

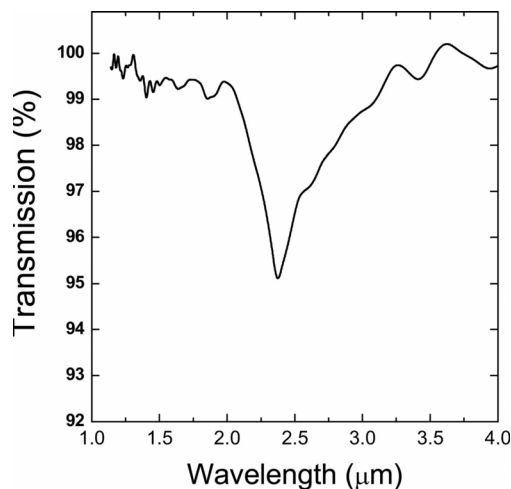


FIG. 2. Transmission spectrum of the 3D photonic structure along the [100] direction.

sults. Simulations were obtained using spherical voxels with refractive index of 1.6 and radius of 250 nm. These simulated voxels may differ with the real ones, which probably present a rather complex refractive-index profile difficult to simulate. The low suppression rate dip in the transmission spectrum could be caused by different reasons including the relatively low refractive-index contrast, the nonuniform voxel shape at different depths caused by the refractive-index mismatch induced aberration, and the scattering caused by the surface roughness of the voxels. A strong improvement of this result could be obtained on two steps: first, by the tailoring of critical writing parameters as the laser wavelength or the pulse frequency, which would favor one photoionization mechanism over others, or would imply different accumulation effects;<sup>20</sup> a second step would be the implementation of an aberration compensation scheme,<sup>21</sup> which could allow writing reproducible submicron voxel structures along much higher depths.

Even though the obtained stop band did not match the optical frequencies of any of the spontaneous emission bands of the  $\text{Nd}^{3+}$  ions, it is of crucial importance to examine the effects caused by the fabrication method on the luminescence properties of  $\text{Nd}^{3+}$  ions inside the photonic structure. The study of the spatial modifications induced in the  $\text{Nd}^{3+}$  luminescence properties provides direct information about the photophysical and photochemical mechanisms at the basis of subwavelength voxel formation. For this purpose, we use a high resolution scanning confocal microscope setup. A pulsed 808 nm laser diode was fiber-coupled to an Olympus BX-41 confocal microscope with a 3D positioning stage mounted on it. Excitation (laser)/emission radiation was focused/collected at room temperature by an Olympus 100  $\times$  UPlanSApo (NA=1.4) immersion oil objective. The spectral properties of luminescence were analyzed by a charge coupled device attached to a fiber coupled 500M SPEX monochromator. The theoretical lateral and axial resolution of the confocal system were estimated to be  $r_{\text{lateral}} \approx 231$  nm and  $r_{\text{axial}} \approx 1038$  nm.

Figure 3(a) shows the luminescence intensity map of a single voxel at first layer. The map displays the luminescence intensity of the  ${}^4F_{3/2} \rightarrow {}^4I_{9/2}$  luminescence band of  $\text{Nd}^{3+}$  ions.<sup>17</sup> A clear decrease in the  $\text{Nd}^{3+}$  luminescence intensity is observed at voxel location. This reduction could be due to the presence of a large density of defects which act as radiation traps. From the measured full width at half maximum (FWHM) of the cross-sectional luminescence intensity profile, a lateral voxel size of 433 nm is obtained, in excellent agreement with CLSM profiles [included in Fig. 3(b) and leading to a FWHM of 495 nm]. Thus, this region could be identified as the directly laser-affected volume consisting of high defect-density and low refractive-index material.

The presence of voxels does not only induce local reductions in the  $\text{Nd}^{3+}$  luminescence intensity but also induces changes in their luminescence spectral shape. Figure 4 shows the room temperature luminescence spectra recorded inside and outside the structure for the two relevant infrared emission bands ( ${}^4F_{3/2} \rightarrow {}^4I_{9/2}$  and  ${}^4F_{3/2} \rightarrow {}^4I_{11/2}$ ) of  $\text{Nd}^{3+}$  ions. Figure 4(b) shows a detail of the emission peak at around 1065 nm. Data included in Fig. 4 have been obtained without perfect confocal conditions and by using a 50 $\times$  MPlan microscope objective (NA=0.75) focused at the center of the 3D photonic structure. As a consequence, the collected lumines-

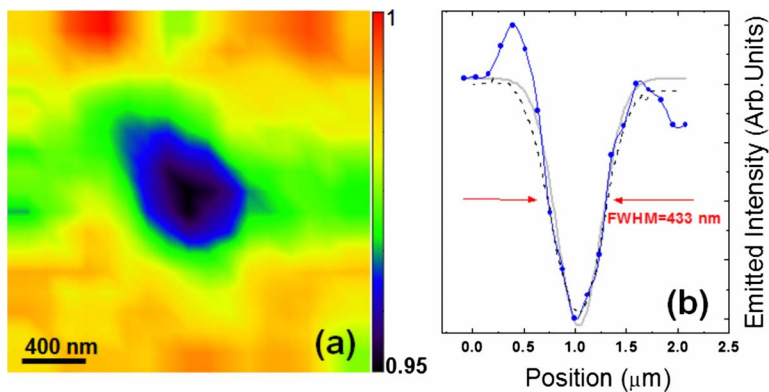


FIG. 3. (Color online) (a) Confocal luminescence image of a single voxel at 6  $\mu\text{m}$  from sample's surface, measured along the [100] direction. (b)  $\text{Nd}^{3+}$  luminescence intensity profile (dotted line) and its corresponding Gaussian fit (continuous line). Also displayed is the lateral CLSM profile of the same voxel as obtained from Fig. 1(b).

cence is generated by  $\text{Nd}^{3+}$  ions located both at the voxels and also in between them. It is clear that a slight line broadening and a redshift of the emission bands have been induced inside the structure. This changes are very likely due to  $\text{Nd}^{3+}$ -ions site redistributions, together with lattice densification, as a result of the tightly focused femtosecond laser pulse processing.<sup>13</sup> Despite these changes, time-resolved luminescence experiments indicate that the luminescence lifetimes of the  $^4F_{3/2}$  metastable state inside and outside the structure are virtually the same (187 and 191  $\mu\text{s}$ , respectively). Thus, the radiation dynamics of the  $\text{Nd}^{3+}$  ions have not been altered within a very short margin, in such a way that  $\text{Nd}^{3+}$  ions located inside the photonic structure preserve their outstanding spectroscopic properties.

In summary, we have fabricated a 3D photonic structure by means of the DLW technique, showing a stop band centered at 2.4  $\mu\text{m}$ , in a Nd:YAG transparent laser ceramic. The submicron voxels constituting the 3D structure have been characterized by a combination of CLSM and confocal luminescence experiments. We have found that the achieved modulation of the refractive index is also accompanied by a slight modulation of the luminescence intensity of neodymium ions located inside the voxel structures. Furthermore, we have also reported on the modifications that the direct laser fabrication process imposes over the spectral and dynamical properties of the Neodymium ions inside the photo-

nic structure. These measurements have not hitherto been reported and provide crucial information for the development of the next generation laser-crystal based photonic devices.

The results here reported also make Nd:YAG ceramics, in combination with the DLW technique, a very promising candidate for expanding the boundaries of applications such as low-threshold lasers, based on the manipulation of the spontaneous emission of the laser active species.

We thank Professor García Solé for fruitful discussions on luminescence analysis. This work was supported by the Spanish Ministerio de Educación y Ciencia (No. MAT-2007-64686), the Universidad Autónoma de Madrid and Comunidad Autónoma de Madrid (No. CCG07-UAM/MAT-1861), and the Australian Research Council (ARC) Centre of Excellence for Ultrahigh-bandwidth Devices for Optical Systems (CUDOS) (No. CE0348259) and ARC Discovery grant (No. DP0665868).

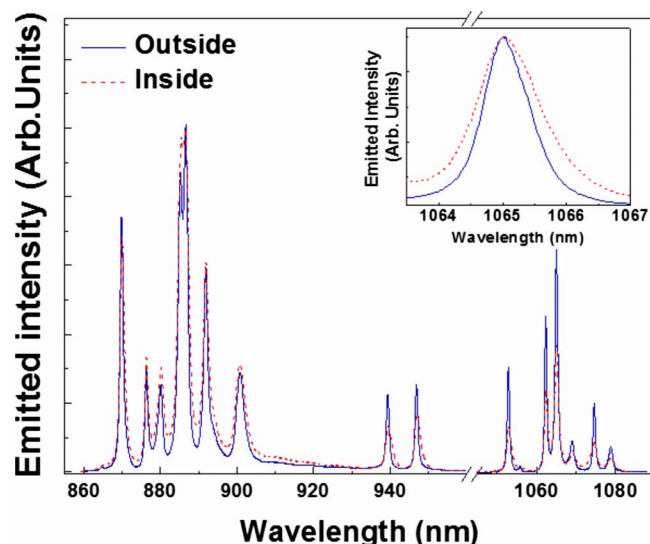


FIG. 4. (Color online) (a) Luminescence spectra of  $\text{Nd}^{3+}$  ions inside and outside the 3D photonic structure. (b) Detail of the normalized 1065 nm emission peak inside and outside the 3D photonic structure.

<sup>1</sup>E. M. Purcell, H. C. Torrey, and R. V. Pound, *Phys. Rev.* **69**, 681 (1946).

<sup>2</sup>E. Yablonovitch, *Phys. Rev. Lett.* **58**, 2059 (1987).

<sup>3</sup>S. John, *Phys. Rev. Lett.* **58**, 2486 (1987).

<sup>4</sup>T. F. Krauss, R. M. De La Rue, and S. Brand, *Nature (London)* **383**, 699 (1996).

<sup>5</sup>O. Painter, R. K. Lee, A. Scherer, A. Yariv, J. D. O'Brien, P. D. Dapkus, and I. Kim, *Science* **284**, 1819 (1999).

<sup>6</sup>M. Campbell, D. N. Sharp, M. T. Harrison, R. G. Denning, and A. J. Tuberfield, *Nature (London)* **404**, 53 (2000).

<sup>7</sup>A. Blanco, E. Chomski, S. Grabtchak, M. Ibsate, S. John, S. W. Leonard, C. López, F. Meseguer, H. Míguez, J. P. Mondia, G. A. Ozin, O. Toader, and H. M. van Driel, *Nature (London)* **405**, 437 (2000).

<sup>8</sup>H.-B. Sun, S. Matsuo, and H. Misawa, *Appl. Phys. Lett.* **74**, 786 (1999).

<sup>9</sup>M. Deubel, G. Von Freymann, M. Wegener, S. Pereira, K. Busch, and C. M. Soukoulis, *Nat. Mater.* **3**, 444 (2004).

<sup>10</sup>H. Misawa and S. Juodkazis, *3D Laser Microfabrication* (Wiley, Weinheim, 2006).

<sup>11</sup>E. G. Gamaly, S. Juodkazis, K. Nishimura, H. Misawa, and B. Luther-Davis, *Phys. Rev. B* **73**, 214101 (2006).

<sup>12</sup>K. Itoh, W. Watanabe, S. Nolte, and C. B. Schaffer, *MRS Bull.* **31**, 620 (2006).

<sup>13</sup>A. Ródenas, J. A. Sanz, D. Jaque, G. A. Torchia, and L. Roso, *J. Appl. Phys.* **100**, 1 (2006).

<sup>14</sup>G. Zhou, M. Ventura, and M. Gu, *Appl. Phys. Lett.* **86**, 011108 (2005).

<sup>15</sup>G. Zhou and M. Gu, *Opt. Lett.* **31**, 2783 (2006).

<sup>16</sup>S. Noda, *J. Lightwave Technol.* **24**, 4554 (2006).

<sup>17</sup>A. A. Kaminskii, *Crystalline Lasers: Physical Processes and Operating Schemes* (CRC, New York, 1996).

<sup>18</sup>J. Lu, M. Prabhu, J. Xu, K. Ueda, H. Yagi, T. Yanagitani, and A. A. Kaminskii, *Appl. Phys. Lett.* **77**, 3707 (2000).

<sup>19</sup>J. Li, B. Jia, G. Zhou, and M. Gu, *Opt. Express* **14**, 10740 (2006).

<sup>20</sup>A. H. Nejadmalayeri and P. R. Herman, *Opt. Express* **15**, 10842 (2007).

<sup>21</sup>M. Gu, *Advanced Optical Imaging Theory* (Springer, Heidelberg, 2000).